Bulletin de l'Institut royal du Patrimoine artistique / Bulletin van het Koninklijk Instituut voor het Kunstpatrimonium

40 | 2025
Varia

Flooded Archaeological Metal Artefacts: Damage Phenomena in Iron Objects from the Centre de Conservation et d'Étude (CCE) in Namur, Belgium

Elke Otten, Helena Wouters and Anne–Sophie Barnich

Electronic version
URL: https://journals.openedition.org/kikirpa/5051
DOI: 10.4000/145sw
ISSN: 2983-855X

Publisher
Institut royal du Patrimoine artistique - Koninklijk Instituut voor het Kunstpatrimonium

Electronic reference
Elke Otten, Helena Wouters and Anne–Sophie Barnich, "Flooded Archaeological Metal Artefacts: Damage Phenomena in Iron Objects from the Centre de Conservation et d'Étude (CCE) in Namur, Belgium", *Bulletin de l'Institut royal du Patrimoine artistique / Bulletin van het Koninklijk Instituut voor het Kunstpatrimonium* [Online], 40 | 2025, Online since 13 May 2025, connection on 19 June 2025. URL: http://journals.openedition.org/kikirpa/5051 ; DOI: https://doi.org/10.4000/145sw

Flooded Archaeological Metal Artefacts: Damage Phenomena in Iron Objects from the Centre de Conservation et d'Étude (CCE) in Namur, Belgium

Elke Otten, Helena Wouters and Anne–Sophie Barnich

Introduction

1 In July 2021, heavy rainfall inundated the entire archaeological storage area of AWaP (Agence wallonne du Patrimoine) and the CCE (Centre de Conservation et d'Étude) in Saint–Servais, Namur, Belgium.[1] Some metal finds came into contact with their greatest adversary: polluted water. In this contribution, we aim to understand the damage inflicted on wrought iron artefacts, the factors that contributed to this deterioration, and formulate options to prevent future damage under similar circumstances.

2 The CCE manages and conserves archaeological materials from excavations in the Walloon Region. Established in 2012, it serves as the central repository for the AWaP. Archaeological materials from various periods, along with excavation plans and archives, occupy approximately 2,000 m² and consist of about 15,000 boxes of combined archaeological materials.

3 On 15 July 2021, within a few hours, muddy waters spread across the entire storage area, reaching a height of 1.5 metres. The small team on–site that day implemented the collection rescue plan prepared for such a disaster: priority collections were evacuated, and the remaining materials were protected as effectively as possible. The CCE metal storages were among the first to be recovered to safeguard priority metal collections.

The boxes containing the archaeological metal materials from the CCE were transferred to another AWaP site on the same day.

4 Regrettably, several factors prevented the evacuation of all the metal archaeological artefacts from the repository as the water level rose. The most significant issue was time. Handling the heaviest and largest items became problematic as mud obstructed the use of trolleys and forklifts. The packaging of the objects also complicated their movement, particularly the long weapons stored on polyethylene foam trays in drawers that could not be dismantled in time (fig. 1). As the lift soon became out of order, it proved challenging to transport the collections upstairs. Consequently, it was decided to relocate what could no longer be extracted from the storage rooms to higher ground. The objects had to be abandoned quickly for safety reasons.

[Fig. 1]

The drawers and conditioning of long weapons in the CCE metal storage before the floods of 2021 (a) and after their recovery (b).

5 From the day after the flood, teams of 25 to 40 individuals, including AWaP staff and volunteers, took turns salvaging their heritage. In the first 48 hours following the initial flood, the metal storage rooms were completely emptied.

[Fig. 2]

Access corridor to the CCE storage areas following the first flood on 15th July 2021.
© Anne–Sophie Barnich@SPW–AWaP.

6 Items not directly affected by the mud but still exposed to high relative humidity were placed in a room quickly arranged to ensure the traceability of the collections and implement the first emergency interventions. Depending on their location in the storage area, the contents of the packing cases were impacted either partially or completely.

[Fig. 3]

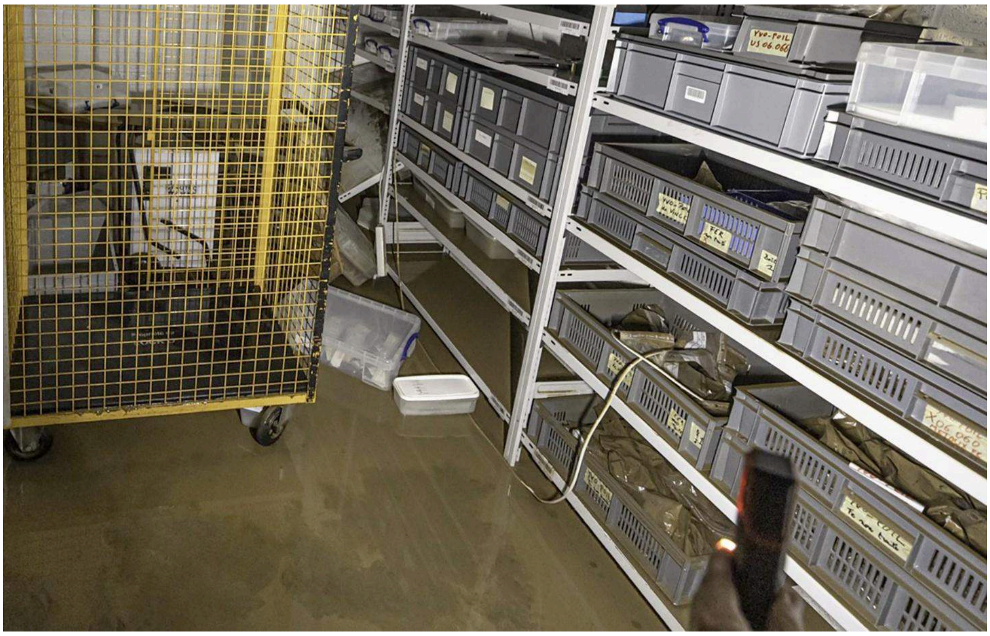

Metal storage room containing crates damaged by mud from the initial flood (15 July 2021).
© Anne–Sophie Barnich@SPW–AWaP.

7 With the assistance of metal conservators and restorers, the affected objects were dried using either absorbent paper or immersion in ethanol. At the same time, archaeological data was recovered to maintain the context of the objects.

8 Some metal objects were stored with other materials in crates within temporary storage rooms, awaiting inventory before being placed in the metal storage. These objects were impacted by the second, even more violent flood that struck the CCE on 24 July 2021.

[Fig. 4]

Second flood that hit the CCE (24 July 2021).

9 Considering the impact of this second flood and the amount of archaeological material affected once again, the decision was made to evacuate all collections to a salvage site provided by the Ministry of Defence. Additionally, an emergency metal storage was created in another AWaP building to better preserve all of the CCE's metal collections under improved conservation conditions.

10 Several scenarios arise regarding metal archaeological objects during such disasters: unaffected materials; indirectly affected materials (high RH); materials impacted by initial flood sludges but preserved due to secure packaging (e.g., tightly sealed crates that floated in muddy waters) and treated urgently; and materials affected by double flooding, which were significantly less well packaged and mixed with other materials. The latter were often placed in perforated cases or cardboard boxes and could be directly placed in containers, bagged, or wrapped in bubble wrap (fig. 5). This factor, along with exposure time to mud and/or uncontrolled drying, substantially influenced the post–flood condition of the metal objects. These observations have led us to question common practices and rethink our choices regarding packaging materials. In addition to these observations, numerous alterations have been documented.

[Fig. 5]

In cases containing metals affected by double flooding, the drying of the case on the left could not be controlled.

11 The artefacts from the CCE were exposed to contaminated floodwater and mud, which, as reported by others, can trigger corrosion within minutes.[2] Despite prior conservation treatments, corrosion can be reactivated on archaeological iron objects even when stored in dry conditions. Since immediate access to the artefacts was not possible, and the effects on the objects could only be assessed after some time, the exact rate of corrosion could not be determined.

12 During the flooding, water and mud reached the artefacts, including those stored in watertight or water–resistant materials (such as sealed plastic bags or airtight containers). Although most objects had undergone conservation treatments after excavation to prevent further degradation, and despite efforts to recover them quickly following the flooding, signs of deterioration were still evident. Using Bertholon's terminology,[3] the surface we will now examine, which we aim to describe in relation to the corrosion phenomena, is neither in its *original state* (the condition in which the object was discarded or abandoned) nor in the condition it was in when recovered, the *excavation condition*. Instead, it reflects the changes that occurred during the *post–excavation* period, influenced by human interventions such as cleaning, consolidation, and other conservation measures, as well as environmental factors during storage and the flood disaster. It is clear that the objects stored at the CCE first corroded during burial were later stabilised by the intervention of conservator–restorers and have now developed new degradation patterns due to water damage over a short period. Visually, the corrosion has been reactivated, intensified, or newly initiated.

13 As observed in the flooded artefacts and noted by Wang,[4] the consolidation products failed to protect the archaeological metal from ongoing corrosion, particularly in the presence of chloride ions. It is well established that the polymers used for consolidation degrade over time, allowing the treated metal to continue corroding and becoming unstable.[5] For instance, Pingitore reported the reappearance of corrosion after a similar conservation treatment was applied to artefacts in the collection, which included mechanical removal of corrosion products, corrosion stabilisation, and consolidation using epoxy resin and acrylic co–polymers.

14 Jaeger indicated that wax coatings, which are also applied to certain objects, do not serve as effective barriers, as humidity and water can penetrate the wax layer. Brüggerhof further noted that epoxy alone is inadequate for protecting iron artefacts affected by chlorides. Even Paraloid®, an acrylic polymer commonly used in conservation for its relative stability against ageing and water–repellent properties, does not consistently provide reliable resistance in humid condition.[6] According to the current metal conservator,[7] these widely used consolidation products were also used to treat the archaeological iron finds from the CCE collection.

15 The question remains whether some surface phenomena observed on the iron can be attributed to the resins and waxes applied during consolidation. The materials used in conservation treatments must not react with the metal substrate or degrade under typical conservation conditions. However, the exceptional occurrence of flooding introduced large quantities of contaminated water and mud into the storage area. The impact of such an extraordinary event on these types of objects is still uncertain and requires further investigation.

Selection of the Corpus

16 From the collection of archaeological metal artefacts transferred for conservation in a dry environment, 17 objects–including keys, fragments of cauldrons, a skimmer, a ladle, and various tools–along with a set of 35 nails, were selected from six different Walloon archaeological sites for research (Annex: Table 1).[8] These items were chosen due to significant changes in their condition following exposure to floodwaters. The changing environmental conditions led to *reactivated corrosion* on the objects or an unstable state. Several physical symptoms, which Loeper–Attia refers to as *post–corrosion,* were observed on the artefacts during a preliminary visual inspection: pitting, cracking, flaking, blistering, and breaking off (fig. 6). Moreover, the brown globules of liquid and the powdery orange–brown corrosion products clearly indicated the chemical alteration of the objects.[9] This degradation is characteristic of iron archaeological artefacts recovered from the soil. The preservation state of iron objects is primarily influenced by burial conditions and various interrelated factors, such as oxygen and water content, salt concentration, and air permeability. Depending on the environmental factors, iron corrosion accumulates in layers. After excavation, the corrosion layers may crack as the iron artefact dries, opening the structure to further corrosion.

17 Most of the ferrous artefacts are not recovered from the soil without decay.[10]

[Fig. 6]

Horseshoe presenting detaching flakes, cracks, blistering and a fragment that broke off, from Wanze Golf.

© Loic Dehogne@SPW–AWaP.

18 On two objects from the archaeological site of Herbeumont Castle, mud was deposited directly onto the treated, yet rough surface and dried in place before a conservator–restorer could intervene.[11] On eight other objects, the presence of mud is limited to a haze or local residues.[12]

[Fig. 7]

Fragment of a tripod cauldron, surface covered with dried mud, from Herbeumont (a) ; Key with local white veil on the surface, from Poilvache (b).

© Loic Dehogne@SPW–AWaP.

19 The white veil on three objects from the archaeological site Poilvache caught attention. This material may suggest a reaction from a conservation material, a soil residue, or a specific type of corrosion.[13]

20 Although packing materials are often chosen with great care for an object's safety, the wrapping of one item from Juprelle led to a problematic situation.[14] The small key was wrapped in cling film, or polyethylene film, which – after the flooding occurred – became stuck to the underlying metal object. In fact, some plastics are known to leach plasticisers over time, potentially adhering to adjacent objects.[15] It remains unclear whether this was the case or if the adhesion resulted from a reaction with the consolidation material.

[Fig. 8]

Fragment of shovel presenting bubble wrap pattern, from Herbeumont Castle (a); Saw blade that adhered to plastic bag, from Herbeumont Castle (b).
© Loic Dehogne@SPW–AWaP.

21 The cling film did not appear to be the only packing material adhered to an object's surface. A fragment of a skimmer and another of a shovel clearly displayed the imprint of bubble wrap on their surfaces.[16] Similarly, the folds of the plastic Ziplock bag were evident on the fragments of the saw blade, originating from the same archaeological site of Herbeumont Castle (fig. 8). The packing materials also showed traces of corrosion products from the objects.[17] In addition to the packing materials, a paper label was discovered on a Herbeumont object after the flooding (fig. 9).[18] It was one of many archaeological items in the flooded storage that could lose valuable reference information if the label was not retrieved.

[Fig. 9]

Fragment of cauldron covered in paper label from Herbeumont Castle.
© Working image and Optical microscopy image 10621.

Macro– and Microscopic Observations

22 As a first step, all selected objects were examined at both macro and microscopic levels to identify surface phenomena related to flooding, previous conservation treatments, and storage conditions.[19] The thin, light brown layer of mud mixed with bright orange corrosion products deposited on top of the inventory number on a gaff hook from Pommeroeul, clearly demonstrates that the flooding initiated changes in the treated object through surface deposits and corrosion reactions of the underlying metal.

[Fig. 10]

Detail of inventory number of a gaff hook from Pommeroeul.
Optical microscopy image 10469.

Observation of Different Corrosion Forms

23 The surfaces of various objects exhibited a wide array of corrosion products with distinct appearances, including powdery materials, granular or crystalline forms, corrosion crusts, and seemingly liquid substances. The following section aims to describe these manifestations.

24 Nearly every selected artefact shows distinct signs of iron corrosion, including rust and patina, marked by orange pitting and the flaking of a metallic layer. The flakes range in size from a few centimetres to several millimetres (fig. 11).

25 Flakes were observed on both the inner corrosion layer and the outer surface. The former is characterised by corrosion oxides that have caused detachment, appearing quite fragile and displaying the typical red–orange hue of rust. The latter refers to the section of the artefact that has been exposed to floodwaters and mud and has undergone restoration. On this side, the density increases, and the colour indicates treated iron.

[Fig. 11]

Flakes detaching from the surface of a horseshoe at Wanze Golf.
Optical microscopy image 10313.

26 The seemingly intact surface of a ladle from Renaud Castle, consolidated with epoxy resin, reveals under magnification that localised corrosion is still occurring beneath the consolidation product.[20] A similar phenomenon, where corrosion emerges from beneath and perforates the synthetic consolidation layer, is observed on the surface of a fragment of a cauldron from Herbeumont.

[Fig.12]

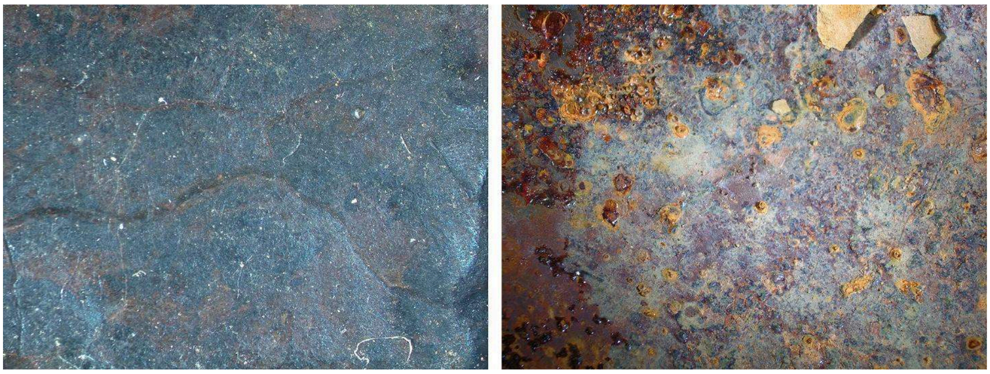

Corrosion beneath the consolidated surface of a ladle from Renaud Castle (a) and Herbeumont Castle (b).
Optical microscopy images 10337 and 10546.

27 The microscopic analysis of this surface further aided the study of the peculiar *stalactiform* corrosion morphology (fig. 13).[21] These elongated particles, which seemed to have grown vertically, formed small columns that resembled the iron oxide

columnar growth observed on an iron artefact by Scott and Eggert, noted for its unusual radial concentric growth cycle features.[22]

[Fig. 13]

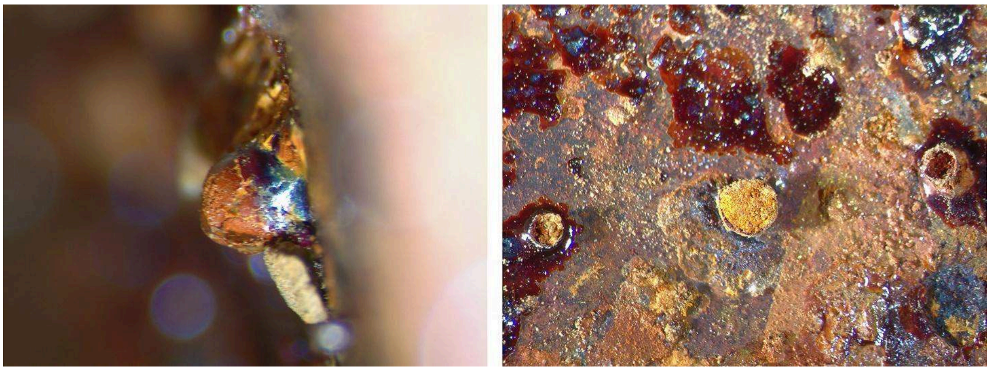

Elongated particles seem to 'grow' from the surface of a cauldron from Herbeumont.
Optical microscopic images 10533 and 10534.

28 As pitting and flaking can be easily seen with the naked eye, the presence of small, dried droplets or hollow spherical shells becomes visible under the microscope. Collectively, the components of the corpus provide insight into the various stages of the so-called weeping of iron: from the liquid droplets of $FeCl_2$ to the dried phase characterised by spherical, fractured shells and the resultant orange-brown columns and curling corrosion products (fig. 14–16). These can be described as polycrystalline, elongated particles with a square cross-section or akaganeite columns.[23] The akaganeite crystals are automorphic; they develop their crystalline form against their surrounding layers, increasing in volume and inducing tensions that lead to the cracking of these layers.[24]

[Fig. 14]

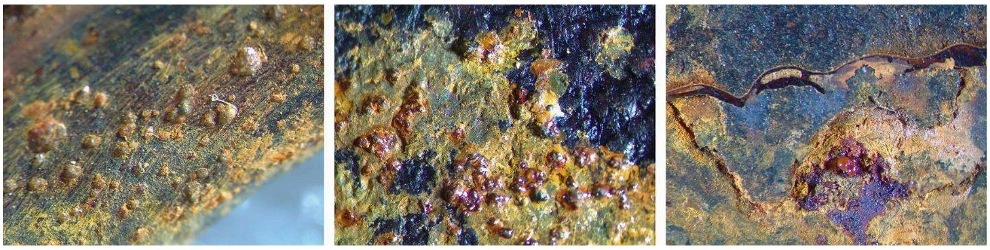

Formation of droplets on 'weeping' iron, on a gaff hook from Pommeroeul (a), a hub from Renaud Castle (b), and on an unidentified object from Wanze (c).
Optical microscopy images 10482, 10368 and 10291.

[Fig. 15]

Broken shells and remnants of droplets on fragments of Herbeumont (a and b) and a key from Juprelle (c).
Optical microscopy images 10548, 10682 and 10515.

[Fig. 16]

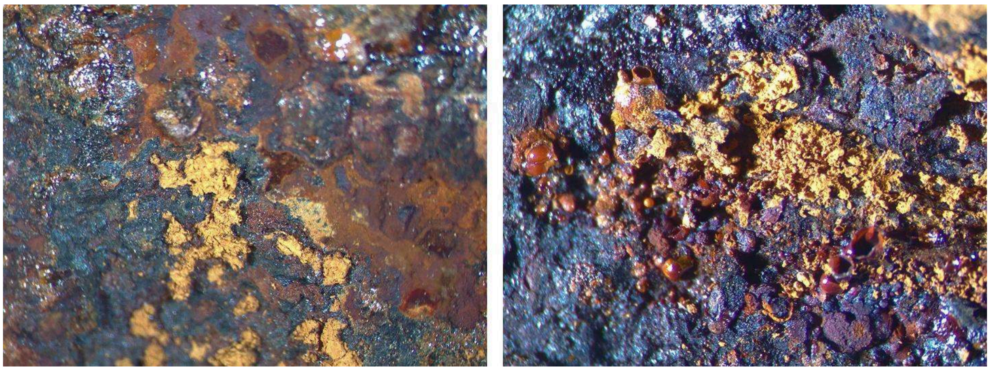

Curly akagaéite particles were observed on a nail from Poilvache (a) and on a key from Juprelle (b).
Optical microscopy images 10436 and 10503.

29 Corrosion products do not cover all strata on submerged archaeological objects. Some surfaces retained mud deposits in microscopic quantities (Renaud Castle CDC–LX–007798) or in thick layers (Herbeumont Castle CDC–LX–007794).

[Fig. 17]

Mud–covered fragment of cauldron from Herbeumont.
Optical microscopy image 10615.

30 Compared to areas without mud deposits, surfaces covered in mud did not appear to experience more severe corrosion. Regions lacking mud were equally susceptible to corrosion (Renaud Castle, CDC–LX–007798). For instance, at the 'hub' of Renaud Castle, the consolidated surface exhibited both bright orange powdery corrosion and hollow

shells, remnants of $FeCl_2$, seemingly in amounts comparable to those seen in the locally affected regions of the mud-covered section of the object.

31 One material, however, found on objects from various sites raises significant questions. It appears on many items as a semi-transparent, shiny orange-brown substance that resembles dried liquid. Identifying this material is essential to determine whether it is related to the droplets and their shells.

[Fig. 18]

Shiny material on a handle from Herbeumont.
Optical microscopy image 10559.

32 The glossy substance appears on heavily corroded surfaces and can be observed leaking from cracks, the edges of flakes, and adhering mud, such as on objects from Wanze and Herbeumont (fig. 19). At times, the substance exhibits cracks that resemble dried liquid (fig. 20).

[Fig. 19]

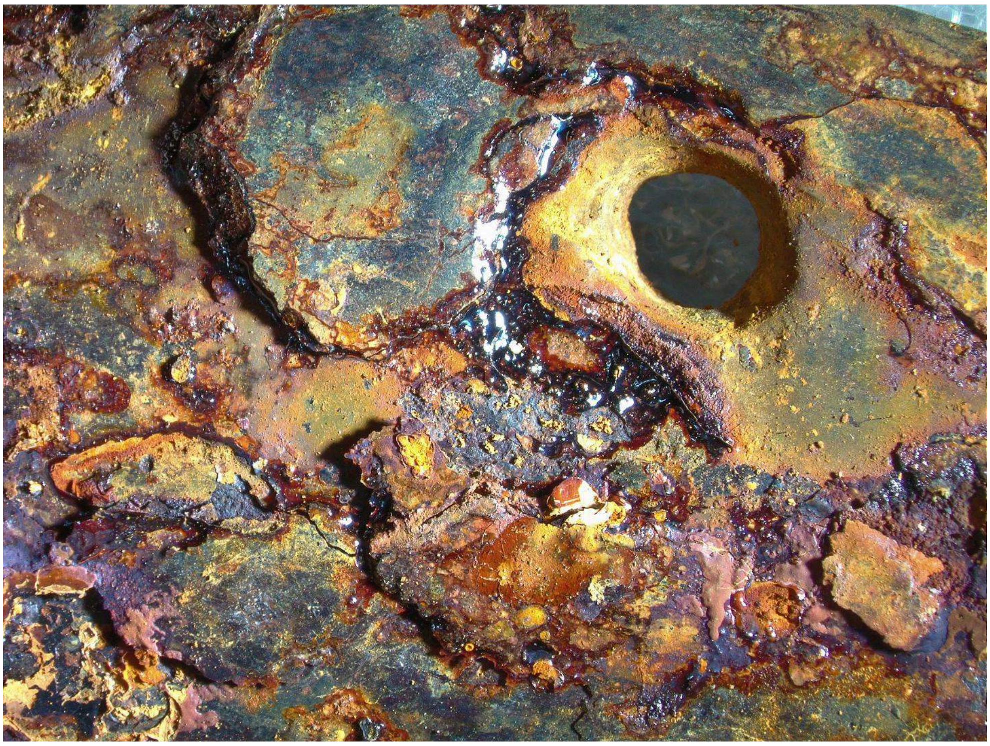

Glossy material found between the flake and the metal core of the horseshoe from Wanze Golf.
Optical microscopy image 10319.

[Fig. 20]

A shiny substance spread across the surface and leaking from a crack in the unidentified object Wanze.
Optical microscopy image 10283.

33 When this material is present in sufficient quantities, it can take on the shape of the packaging that surrounds the object. The folds of plastic Ziplock bags and the patterns of bubble wrap are clearly imprinted and visible. For instance, on the shovel, the upright rims around the bubbles remain on the surface, and within these round shapes, bright orange powdery corrosion is evident where the bubbles would have made contact with the object (fig. 21–22).

34 The shiny substance also adhered to the bubble wrap, Ziplock bags, or cling foil packaging, whether small fragments from the Herbeumont skimmer were attached to it or larger pieces were on the Ziplock bag (fig. 23).

[Fig. 21]

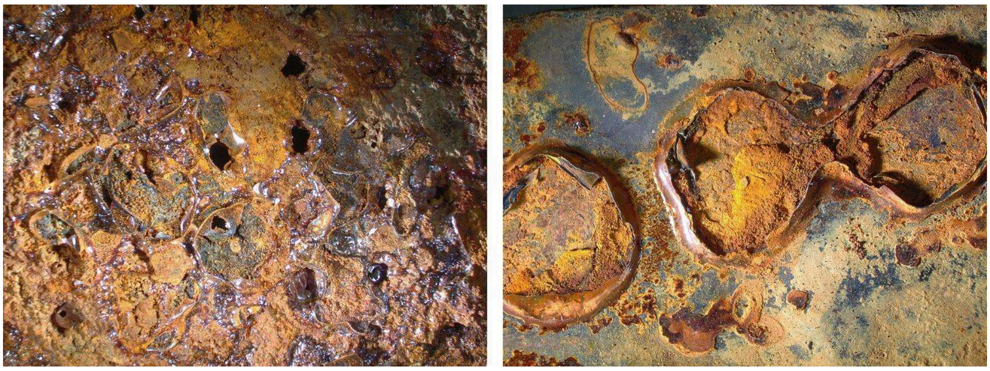

The imprint of bubble wrap is visible on the surface of a skimmer from Herbeumont Castle and on a fragment of a shovel from the same site.

Optical microscopy images 10568 and 10594.

[Fig. 22]

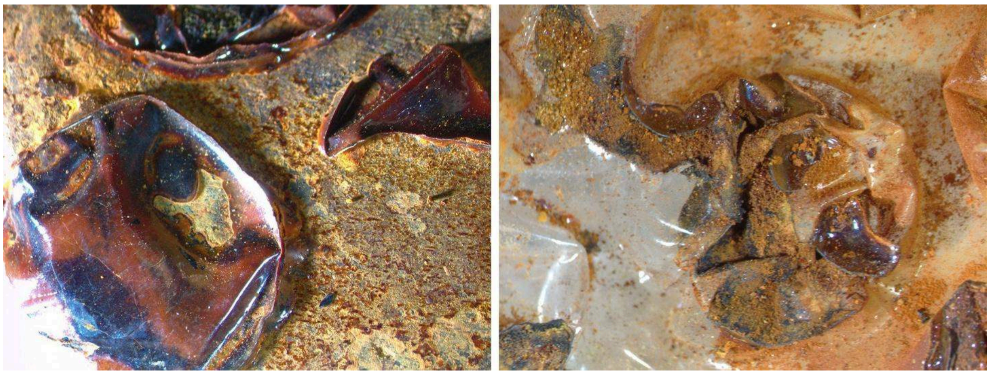

Powdery corrosion is visible along the shiny rim where the bubble wrap touched the metal surface of Herbeumont Castle. Material residue can be observed on the bubble wrap from Herbeumont Castle.

Optical microscopic image, 10595 and 10571.

[Fig. 23]

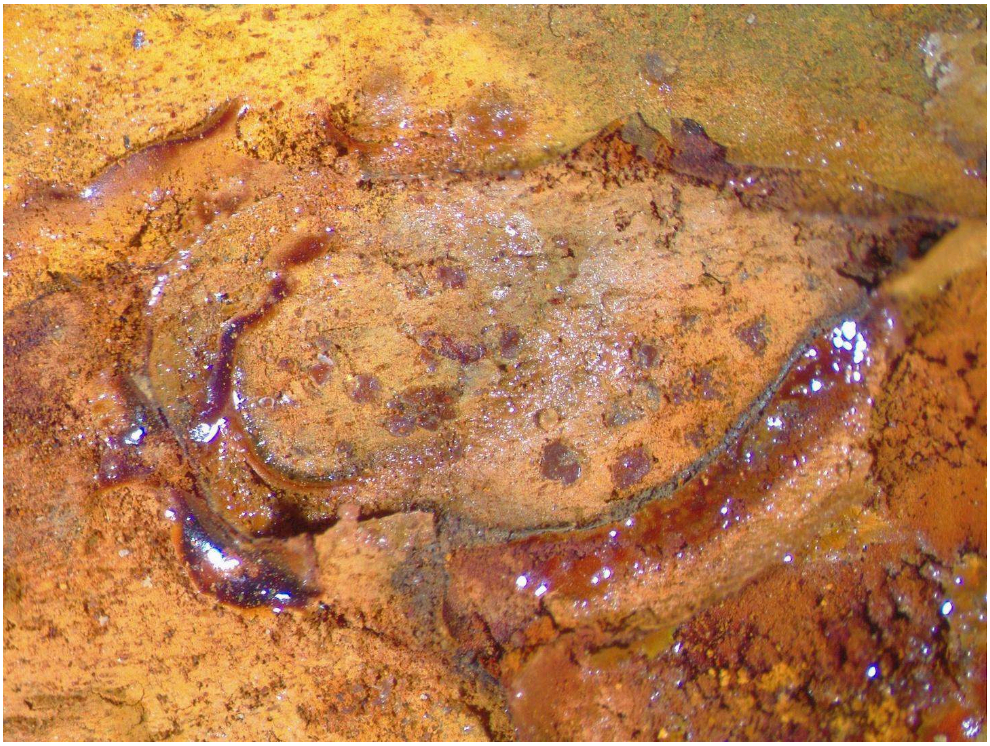

Imprint of a Ziplock bag on the surface of a saw blade from Herbeumont Castle, along with a detail of the shiny substance.
Optical microscopy image 10645.

35 The shiny material appeared alongside a matte, discontinuous light orange crust on the surface of a shovel blade, as well as a fragment of a cauldron from Herbeumont, exhibiting a dry and powdery consistency (fig. 24). Locally, the powder formed rounded granules and globules of various sizes.[25] This crust of globular particles is cracked and stained with the shiny material, which seems to have developed beneath and been deposited atop this layer. This indicates the presence of a layer of deposits combined with corrosion products.

[Fig. 24]

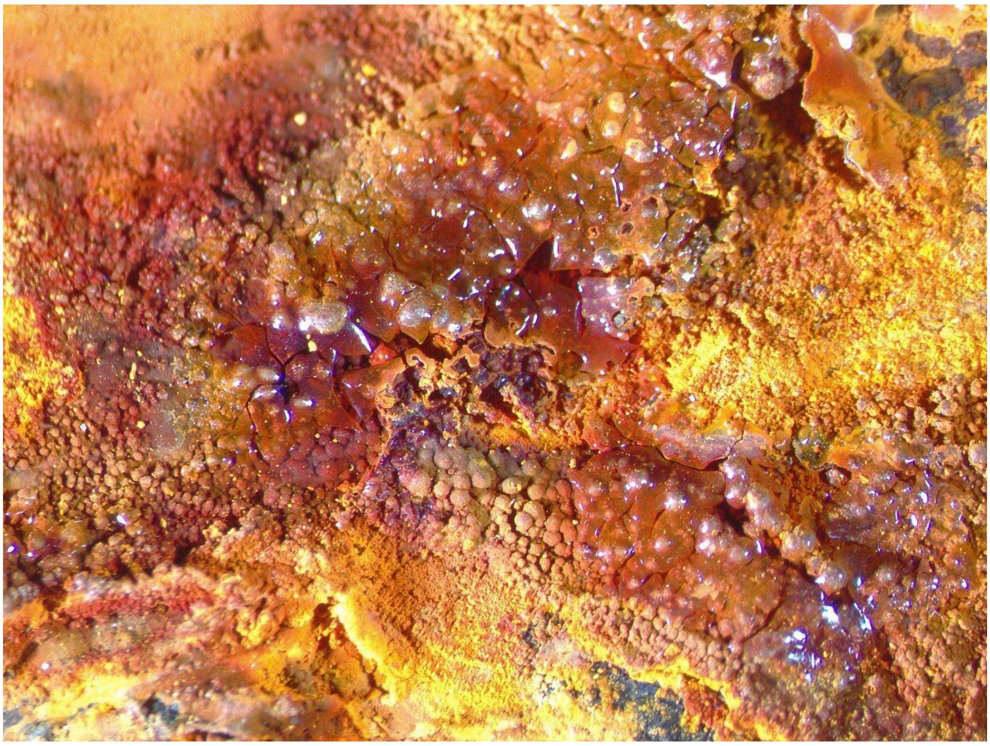

A light orange crust with globular particles observed on a shovel from Herbeumont Castle.
Microscopic image 10609.

36 The reason the liquid is clearly present in a larger quantity than, for example, the liquid from the iron chloride droplets remains to be examined. Its composition requires identification to determine whether it is a corrosion product or a by-product related to the corrosion process resulting from the iron's weeping, a consolidation material leaching from the object's surface, or a mixture of both. Furthermore, the interaction that occurred between the iron metal, conservation material, and packing material also needs identification. At this point, it is still unclear whether, or to what extent, the flooding and conservation conditions contributed to its formation.

Observation of White Deposits

37 A thick white crust is visible on two keys of Poilvache (fig. 25). These deposits appear locally on the surface and consist of a dull, white, *botryoidal* material that can be seen without magnification.[26]

[Fig. 25]

White crust on key from Poilvache.
Optical microscopy image 010413.

38 Most other white substances were visible only under the optical microscope. Their morphology differed significantly from the initial study of the white crust. On a fragment of a cauldron (Herbeumont), scattered across the orange corrosion layer and seemingly emerging from these corrosion products, a drusy aggregate of tiny needles or fine elongated white crystals with wedge–shaped tips could be observed (fig. 26). These were also found on a second object, a saw blade from the same site in Herbeumont. However, alongside the crystal needles, another type of crystal was present on the same saw, which was more granular in nature and consisted of white cubic particles. The nature of these crystals is visually challenging to identify (fig. 27).

[Fig. 26]

Drusy aggregates of small white needles on a cauldron fragment from Herbeumont.
Optical microscopy image 10637.

[Fig. 27]

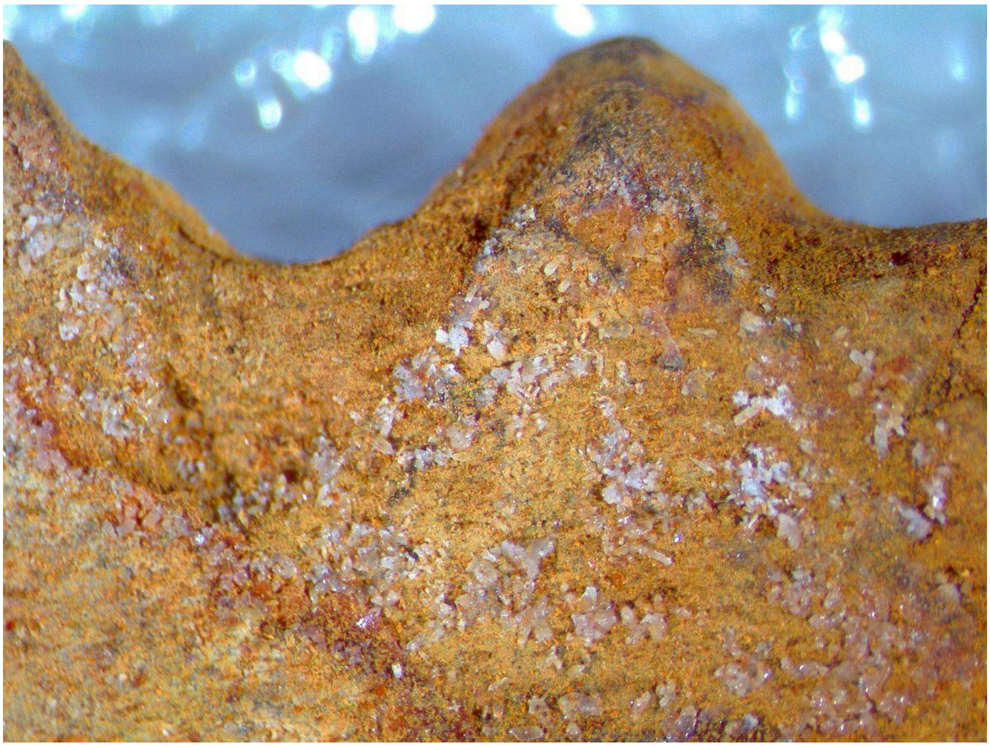

White needles and cubic particles on a saw blade from Herbeumont.
Optical microscopy image 10651.

39 Seven other objects exhibited white particles that were equally challenging to identify. [27] On a fragment of a cauldron from Herbeumont, these somewhat cubic–shaped white particles specifically appear in the transition zone between the unaffected metal and the part that was affected, almost indicating the water line (fig. 28–29). Microscopic examination of these particles alone was insufficient to determine whether they are a deposit from the flood water, mud, or a conservation material used on the objects.

[Fig. 28]

Details of the deposits found on fragments of cauldrons from Herbeumont.
Optical microscopic images 10701.

[Fig. 29]

Deposit of white cubic particles located at the waterline of a cauldron's foot from Herbeumont.
Optical microscopy image 10709.

Discussion

Mechanisms of Active Corrosion: Weeping and the Formation of Akaganeite Corrosion

40 The macro– and microscopic observations clearly assessed the reactivation of corrosion in various forms on the surfaces of previously conserved iron artefacts. Notably, the presence of liquid droplets and spreads, as well as thin spherical hollow shells of solid material, has been observed. Archaeological conservators refer to this phenomenon as 'weeping'. Initially, it was associated with the formation of droplets of $FeCl_3$.[28] However, research in the early 1980s revealed that the liquid predominantly contains Fe^{2+} ions, with relatively low amounts of Fe^{3+} ions and significant concentrations of Cl^{-} ions. Nonetheless, the minimum relative humidity at which weeping may occur has not been conclusively determined.[29]

41 The formation of shells can be explained as a result of the oxidation and hydrolysis of Fe^{2+} ions or the hydrolysis of Fe^{3+} ions, leading to the precipitation of FeOOH in liquid droplets. Several forms of solid iron oxyhydroxides are known: Goethite (α–FeOOH), the most thermodynamically stable; Lepidocrocite (γ–FeOOH); and Akaganeite (β–FeOOH). The latter is rarely found in nature but is often detected on untreated archaeological iron exposed to air. The colour of all these iron oxyhydroxides is influenced by particle size and shape, resulting in various shades of yellow, orange, red, or brown.

42 The SEM–EDX analysis[30] of samples from the hollow shells of weeping iron, collected from the Juprelle object, as well as from objects 007795 and 007797 in Herbeumont, and object 005279 in Pommeroeul, is presented in figures 30–34. For this analysis, a small droplet was taken from the surface and placed onto a support in the SEM–EDX sample chamber. In the case of the broken piece of the saw blade (object 007797, Herbeumont) that was attached to the inside of the packaging bag, the entire fragment was placed in the sample chamber of the electron microscope. In the figures, the black and white image (on the left) represents the backscattered electron image of the sample. All coloured images combined in figures 30–34 illustrate the elemental distribution patterns of the droplet and the corrosion areas of iron (Fe), carbon (C), oxygen (O), chlorine (Cl), sulphur (S), and phosphorus (P). It can be observed that the droplet itself is primarily composed of Fe and O, while chlorine is more concentrated in the layer below. The presence of phosphorus (fig. 34) was only detected in this specific sample and is interpreted as potentially resulting from external contamination.

43 It is evident, especially in figures 30 and 32, that several polycrystalline particles have formed beneath the fractured shells and appear to be mainly composed of iron and oxygen.

[Fig. 30]

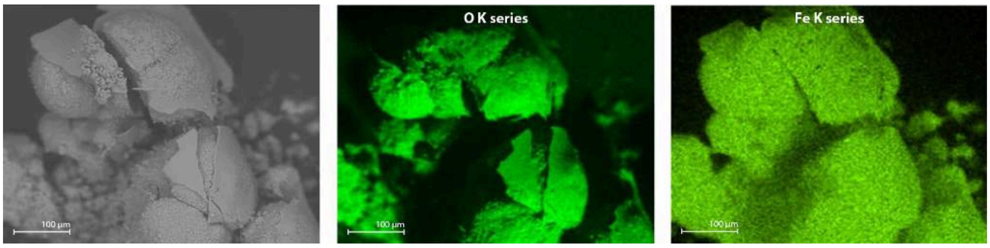

The backscattered electron image, along with the distribution patterns of oxygen (O) and iron (Fe), was obtained through SEM–EDX analysis of a broken shell sourced from the surface of a saw blade from Herbeumont (CDC–LX–107797).

[Fig. 31]

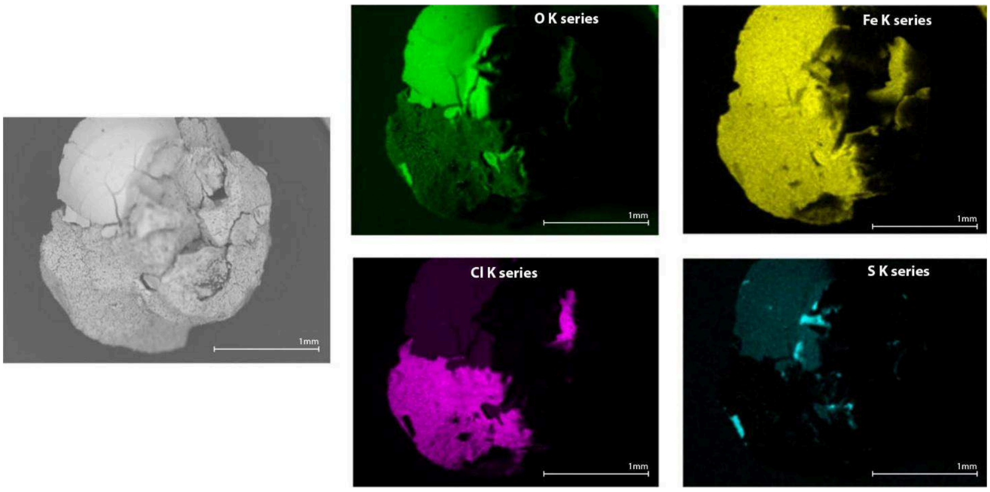

The backscattered electron image, along with the elemental distribution patterns of oxygen (O), iron (Fe), chlorine (Cl), and sulphur (S), was obtained through SEM–EDX analysis of a shell separated from a key found in Juprelle (CDC–LG–023380).

[Fig. 32]

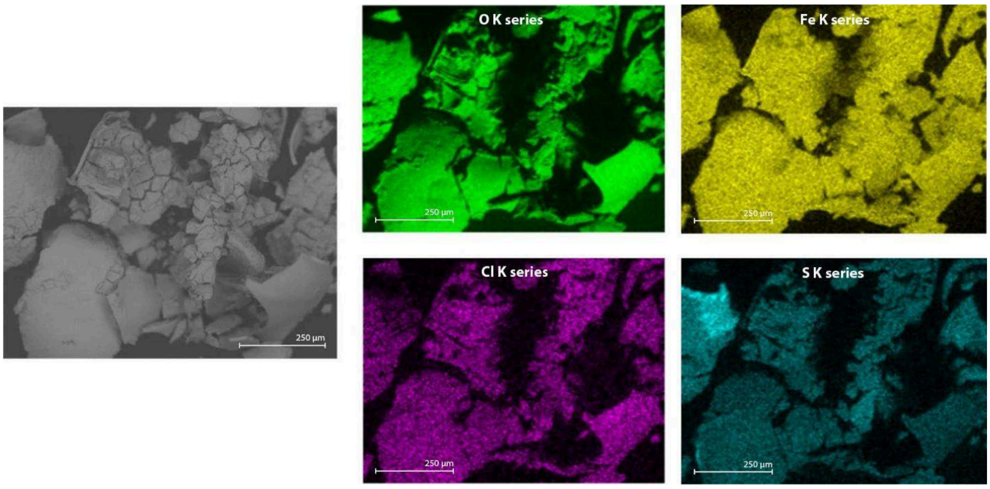

Backscattered electron images and element distribution patterns of oxygen (O), iron (Fe), chlorine (Cl), and sulphur (S) were obtained through SEM–EDX analysis of a chipped flake from a gaff hook found in Pommeroeul (CDC–HT–005279).

[Fig. 33]

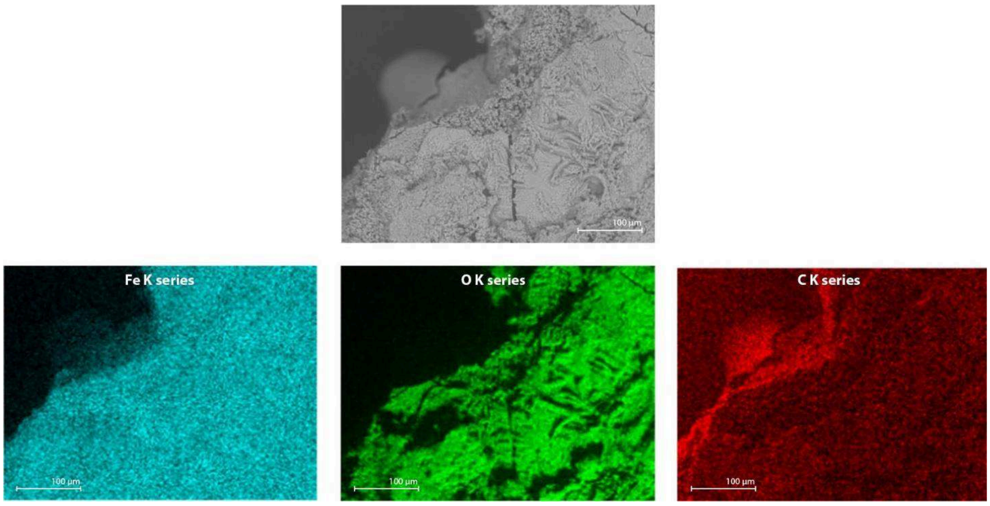

Backscattered electron images and the elemental distribution patterns of iron (Fe), oxygen (O), and carbon (C), obtained through SEM–EDX analysis of a chipped flake from a shovel at Herbeumont Castle (CDC–LX–007795, sample 4).

[Fig. 34]

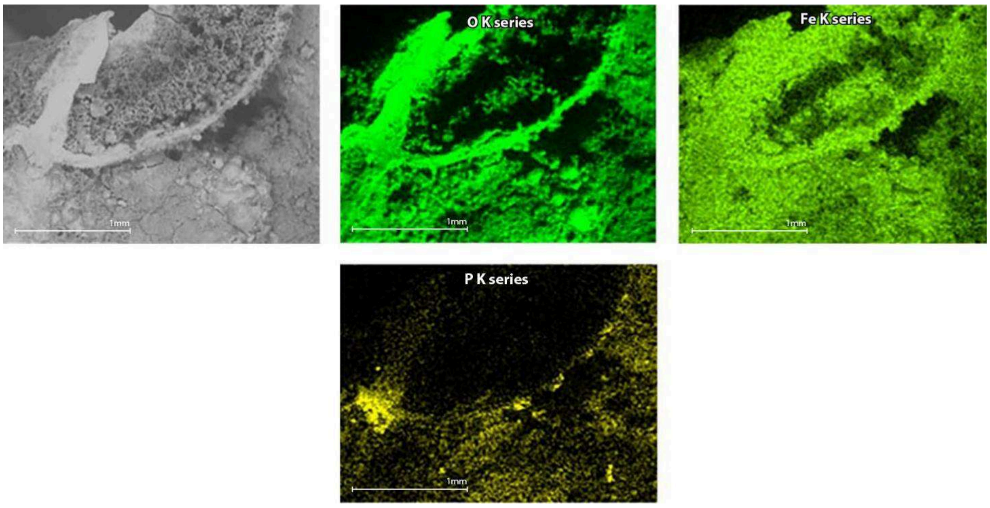

The backscattered electron image and the elemental distribution patterns of oxygen (O), iron (Fe), and phosphorus (P) were obtained through SEM–EDX analysis of a broken piece of the saw blade lodged inside the packaging bag (Herbeumont, CDC–LX–107797).

44 Chloride ions, along with sulphates, are known to accelerate the rusting of iron, but not in all circumstances. However, unlike Cl ions, sulphate ions are gradually removed from the corrosion cycle because they form insoluble iron(III) hydroxysulfates; consequently, the corrosion cycle cannot proceed as it normally would.[31] The chlorine corrosion cycle, on the other hand, occurs only as long as there is free access to oxygen on the iron surface contaminated with an acidic solution containing Cl ions. This acid regeneration cycle explains why excavated iron is rapidly destroyed when exposed to air. If, however, the corrosion cycle leads to a buildup of iron oxyhydroxides (FeOOH), the oxygen supply to the metal surface may become limited, and the corrosion rate will decrease. Of course, other reduction reactions that allow corrosion to continue may also come into play.

45 When water is removed from an iron(II) chloride solution, hydrated salt crystals (like $FeCl_2 \cdot 4H_2O$ or $FeCl_2.2H_2O$) form. These salts are hygroscopic, able to draw moisture from the air above a 'critical RH' typical for that salt. Because they are water–soluble, they can absorb enough moisture from the air to dissolve completely and create a solution.

46 Although Turgoose[32] suggested that weeping occurs away from the metal surface, the SEM–EDX analysis of the cross–section of the lifted sample from object 023379 of Wanze (fig. 35) allowed us to observe weeping starting from the metal surface and then extending outward above the corrosion layer, as also indicated by Selwyn[33].

[Fig. 35]

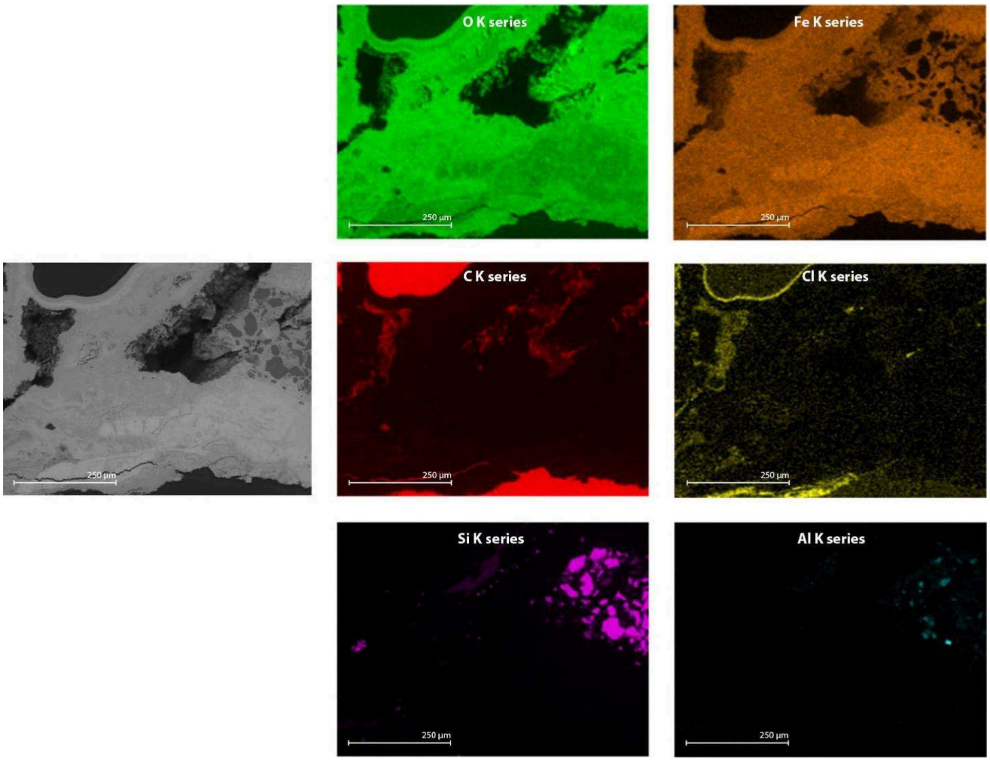

Backscattered electron image, along with the elemental distribution patterns of oxygen (O), iron (Fe), carbon (C), chlorine (Cl), silicon (Si), and aluminium (Al), was obtained through SEM–EDX analysis of a sample taken from the cross–section of a horseshoe from Wanze Golf (CDC–LG–023379).

47 To determine the type of iron oxyhydroxide formed on the surface of corroded iron objects, µRAMAN analysis was used.[34] The studies and findings reported by researchers Neff and Réguers informed the selection of optimal analysis parameters.[35]

48 As shown in figure 36 for a sample of Pommeroeul and in figure 37 for a sample of Juprelle, the results align excellently with the β–iron oxyhydroxides (akaganeite) spectrum obtained from the synthesised powder in the study by Réguer *et al.*[36] Indeed, in the low–wavenumber region (FeO stretching vibrations and FeOH bending vibrations), the spectra reveal three intense, broad bands at 310, 390, and 720 cm^{-1}. The slight differences between the spectra can be attributed to various factors: grain size, crystal orientations, or differing Cl content.

[Fig. 36]

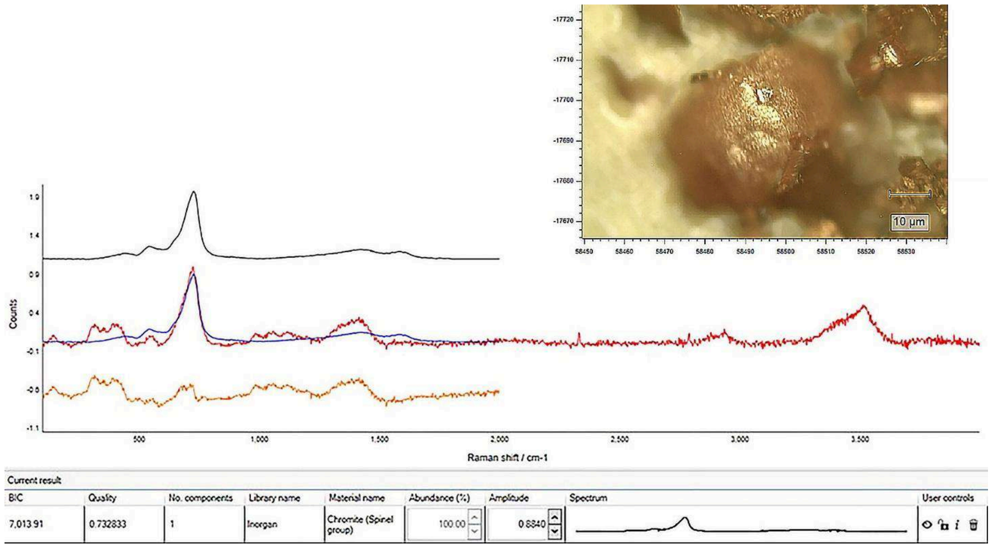

RAMAN results for a chipped flake of a gaff hook from Pommeroeul (CDC–HT–005279, sample 1) were recorded with the laser at 532 nm (Laser power: 1% (max 50 mW); Exposure time: 900 s; Accumulations: 1).

[Fig. 37]

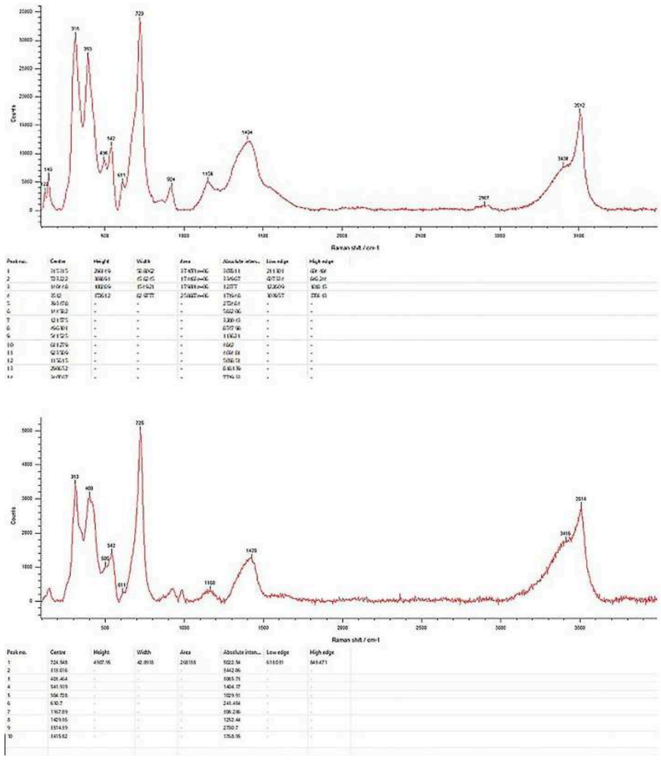

The Raman spectrum of a separated shell adhered to the package foil of a key from Juprelle (CDC–LG–023380) shows that the obtained Raman band positions indicate the presence of akaganeite (Laser power: 0.1875% (max 50 mW); Exposure time: 900 s; Accumulations: 1; Laser: 532 nm).

49 The extensive crystal formation of these iron oxyhydroxides induces significant stress within the artefact, particularly along the corrosion interface. Such stresses can lead to complete delamination or spalling of the outer layers, resulting in the separation of

these outer layers from the core of the artefact, or even total disintegration.[37] Consequently, the cracks facilitate easier access for oxygen and moisture, allowing the chloride corrosion cycle, as documented in the literature for freshly excavated iron artefacts, to persist.[38]

50 In addition to the occurrence of akageneite, another iron corrosion product was identified through µRAMAN analysis of a fragment from the cauldron body (object 007794, sample 2, Herbeumont). The results presented in figure 38 align with the presence of pyrrhotite, an iron sulphide ($Fe_{(1-x)}S$, where x ranges from 0 to 0.2).

[Fig. 38]

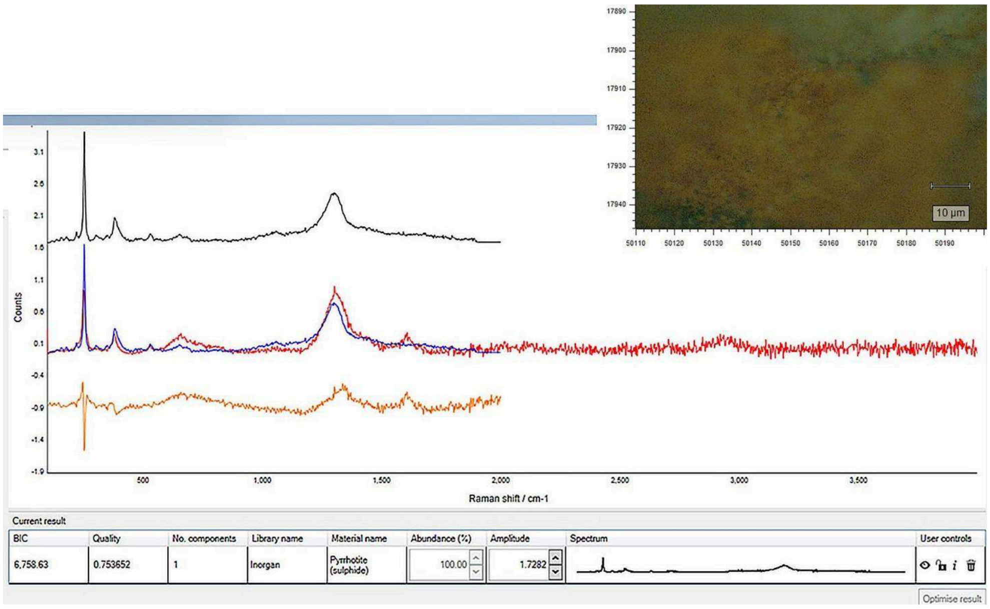

RAMAN results for sample 2–1 (orange material) taken from a fragment of a Herbeumont cauldron (CDC–LX–107794) ; (Laser power: 0.1% (max 50 mW); Exposure time: 900 s; Accumulations: 1; Laser: 532 nm).

51 Pyrrhotite is the second most abundant iron sulphide after pyrite (FeS_2).[39] The formation of iron sulphides occurs when iron artefacts are exposed to hydrogen sulphide, which results from the putrefaction of organic sulphur compounds or from the activities of sulphate–reducing bacteria under anaerobic conditions.[40] Most of the Herbeumont artefacts were covered by a very thick layer of mud, known for its sulphur–rich environment. Therefore, the presence of pyrrhotite is highly plausible. This becomes even more credible as Lara’s study shows that weathered pyrite samples do not generate secondary compounds.[41] In contrast, variable amounts of iron oxyhydroxides and elemental sulphur compounds were identified in the weathered pyrrhotite samples. The co–occurrence of akageneite and pyrrhotite found in the Herbeumont artefacts confirms these findings.

52 Establishing the relationship between the corrosion products on the objects and the soil in which they were buried presents challenges for this corpus. This is because the artefacts were excavated a long time ago and have since remained in archaeological storage. The soil parameters that primarily contribute to corrosion in objects are unknown; however, they are crucial for determining the type of corrosion that occurs on the metal. [42]

53 The conservation records are no longer traceable.[43] The salvage treatments, applied during times of distress when conservators and volunteers work under emergency conditions, are only partially documented, primarily after the crisis. The same sequence of events was observed by the team working on the flooded metal collection of the Musée Girodet in Montargis.[44] This complicates establishing a clear connection with earlier conservation treatments. Furthermore, no conservation products were detected through Raman analysis. This also aligns with the experiences of conservators dealing with the Montargis flooding, who noted that protective layers of wax and varnish seemed to have washed off the metal objects in a very short time during the flooding.[45]

54 Examining the overview in the Appendix (Table 1), it appears that the time between flooding and relocating an object to suitable, dry conditions is less critical than the exposure to extreme humidity or wet conditions. Once an object is flooded, corrosion seems to reactivate without any clear distinction. In contrast, the artefacts being conserved and stored in plastic seem to have influenced the potential damage following the flooding. At this point, it remains uncertain whether the transparent material would similarly affect other iron artefacts after water damage. It is essential to consider the packaging of items, such as Ziplock bags, polythene film, and hermetic plastic containers. These could provide an additional barrier against water, alongside the building envelope and storage furniture, and are therefore recommended.[46] In the case of flooding on this scale, they would not prevent the objects from becoming wet from the water.

55 The decision to use plastic materials should be well–informed, just like other materials introduced in the storage area. Williams suggests a 'risk–benefit' analysis, considering the vulnerability of the artefacts and the potential risks involved.[47] The risk of leaving a bubble wrap pattern on objects is already clear and is included in practical guidelines, such as the Fact Sheet from the Society for Museum Archaeology. When using bubble wrap, regardless of the observed reactions between different materials, it is crucial to follow the basic rule of placing the smooth side of the wrap toward the object and ensuring that the bubbles never come into contact with it.[48] However, studying the Namur corpus reveals that plastic wrapping of any kind can leave imprints on the object's surface through the folds in the shiny, solidified corrosion liquid.

Occurrence of Ca–rich Deposits, Tiny White Needle Crystals and White Cubic Particles

56 Of particular interest is the white powdery substance found on objects from the archaeological site of Poilvache. Bertholon[49] has noted that these deposits indicate the nature of dissolved elements or biological activity in the environment surrounding the object. They are closely related to the sediment and sometimes to the archaeological context, providing evidence of the object's use. In certain archaeological contexts, such as demolition fills, it can be challenging to distinguish between plaster–based coating fragments that may have accidentally come into contact with the object and calcium sulphate deposits that formed in direct contact with it.

57 In this regard, the white powder taken from one of the keys associated with the Poilvache recoveries (object 015625) was analysed using SEM–EDX and µRAMAN. The elemental results indicate the presence of calcium (Ca), carbon (C), and oxygen (O),

which µRAMAN analysis confirmed as chalk (calcium carbonate), as shown in figures 39 and 40.

[Fig. 39]

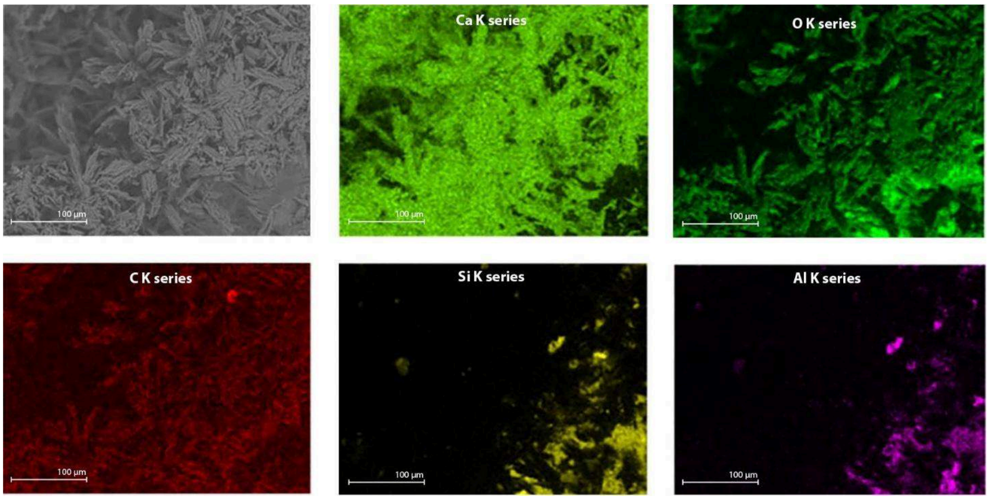

A backscattered electron image, along with the elemental distribution patterns of calcium (Ca), oxygen (O), carbon (C), silicon (Si), and aluminium (Al), was obtained through SEM–EDX analysis of the white crust on a key from Poilvache (CDC–NR–015626, sample 2).

[Fig. 40]

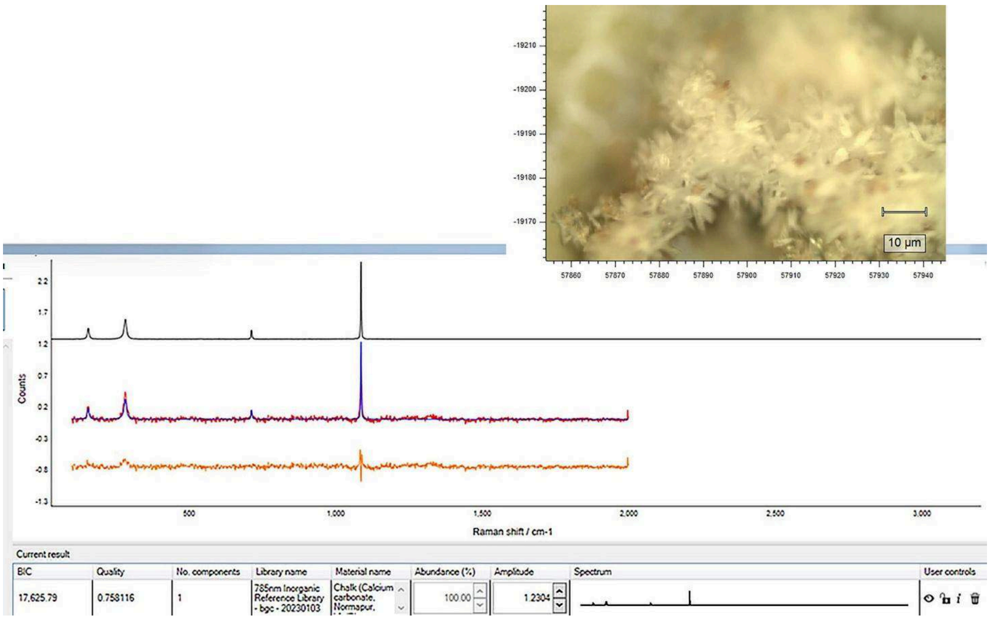

Raman analysis results for the white crust on a key from Poilvache (CDC–NR–015626, sample 2.5): (Laser power: 1% (max 50 mW); Exposure time: 10 s; Accumulations: 5; Laser: 785 nm).

58 Additionally, other structures were found, including small white grains, cubes, and needles. It is suggested that these formations may originate from the conservation materials, which seem to have changed due to the floods or environmental conditions. This is a plausible hypothesis that requires further investigation.

59 A cross–section of an orange, powdery flake from key 015625 of Poilvache was prepared to examine both the 'ancient inner corrosion layer' and the 'outer surface' in hopes of

revealing any prior conservation treatment. The element distribution patterns obtained from SEM–EDX analysis are presented in figure 41. The measurements indicate that one side of the metal has a silicon (Si) rich zone, likely due to the presence of mud, sand, or dirt. A distinct calcium (Ca) rich layer adjacent to the metal is also observed. On the opposite side of the metal, a thin chlorine (Cl) rich layer and a sulphur (S) rich portion are noted. Thus far, a possible organic layer indicative of a previous treatment has not been found.

[Fig. 41]

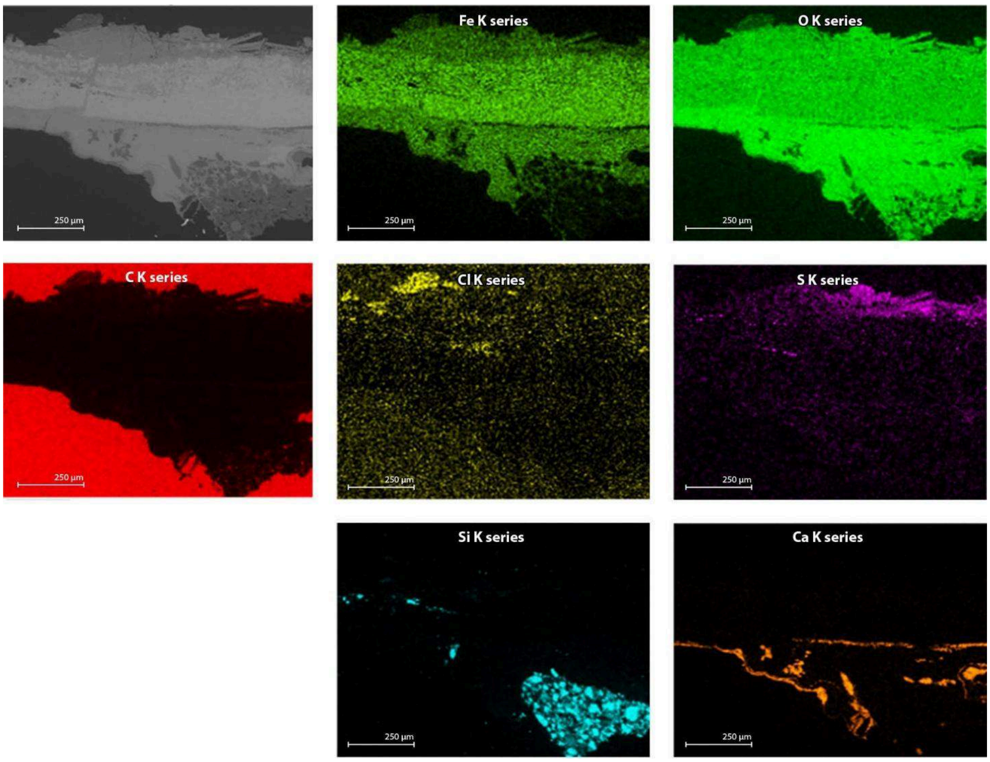

The backscattered electron image, along with element distribution patterns of iron (Fe), oxygen (O), carbon (C), chlorine (Cl), sulphur (S), silicon (Si), and calcium (Ca), were obtained through SEM–EDX analysis of a cross–section from a sample taken from an orange powdery flake of a key from Poilvache (CDC–NR–015626).

60 In another step of the study, a small white grain lifted from a separated flake of the saw (object 007797, Herbeumont) that was attached to the plastic bag, was moved to FTIR analysis[50]. The spectra presented in figure 42 closely align with calcite, as evidenced by the pink line representing the reference spectrum of calcite.

[Fig. 42]

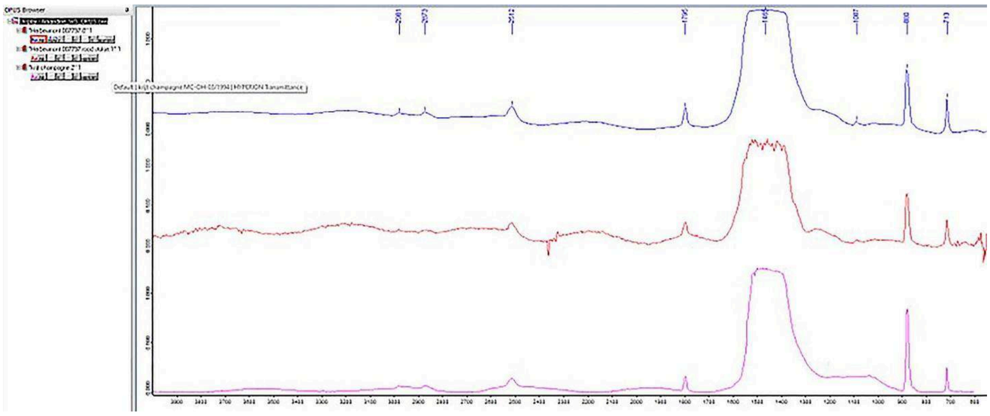

FTIR spectrum of a white grain extracted from the surface of a flake of the saw (object 007797, Herbeumont). The blue and red lines correspond to the sample, while the pink line represents the reference spectrum of calcite.

Conclusions

61 The damage and contributing factors to the deterioration of iron artefacts from the flooded archaeological storage area of the CCE in Namur were studied. Particular attention was given to understanding the interaction between metal corrosion and the materials used to package the archaeological objects, as well as the influence of previous conservation treatments.

62 Both macroscopic and microscopic examinations revealed typical orange pitting and exfoliation of the metallic layer. Additionally, spherical and fragmented shells of dried droplets, along with formations of liquid and dried phases, as well as orange–brown columns or curly corrosion products, were identified on the damaged iron surfaces. Particularly on objects wrapped in bubble wrap, the thin layer formed during the 'weeping iron' process assumed extreme forms. Unusual, elongated particles, which appeared to grow upwards in a *stalactiform* corrosion morphology, were also observed. These observations clearly indicate the physical damage caused by bubble plastic packaging.

63 The identification of the newly formed corrosion products can be assessed by applying SEM–EDX, µRAMAN, and FTIR analyses. The composition of the dried droplets and liquid/dried phase appears to consist of the active corrosion product β– iron oxyhydroxides (akageneite). The liquid/dried appearance results from the weeping process of iron under specific conditions.

64 In the case of the Herbeumont artefacts, many of the objects were coated with a thick crust of mud typical of their sulphur–rich environment, indicating the presence of pyrrhotite (a member of the iron sulphide group).

65 Of particular interest is the white powdery substance found on objects from the archaeological site of Poilvache. The powder was identified as chalk, a form of calcium carbonate. Additionally, unusual white deposits were observed on the Herbeumont artefacts. While these observations suggest that the appearances may stem from conservation materials likely affected by floods or environmental conditions, analysis confirmed only the presence of calcite, another variant of $CaCO_3$.

66 The study concludes that none of the previous treatments or packaging systems withstood the impact of the extreme flooding. Furthermore, no trace of treatment products was found. In addition to the physical damage caused by the bubble wrap, there was no chemical interaction between the plastic and the artefacts. The dried droplets and broken circular liquid–dried shells resulted from the significant, large–scale impact of the iron's weeping process, which was intensified by the chlorine–rich environment.

67 This study highlights the necessity of reevaluating packaging materials for storage and underscores the importance of creating strategies to avoid similar damage in future events.

We are immensely grateful to Cristel Cappucci (AWaP) for providing invaluable information that enhanced our understanding of the potential former treatments of the objects.

BIBLIOGRAPHY

Barnich 2022 A.–S. Barnich, *Le Centre de Conservation et d'étude (CCE) des biens archéologiques wallons évacué*, in *La Lettre Du Patrimoine*, 65, 2022, p. 6–7.

Bertholon 2000 R. Bertholon, *La limite de la surface d'origine des objets métalliques archéologiques. Caractérisation, localisation et approche des mécanismes de conservation*, PhD thesis in Humanities and Social sciences, Université Panthéon–Sorbonne–Paris I, 2000.

Brokerhof, Ankersmit and Ligterink 2017 A. Brokerhof, B. Ankersmit and F. Ligterink, *Risk Management for Collections*, Rijksdienst voor het Cultureel Erfgoed, Amersfoort, 2017.

Brüggerhoff, Eggert and Simon 2009 S. Brüggerhoff, G. Eggert and S. Simon, *Salze im Museum und in der Archäologie*, in H.–J. Schwarz and M. Steiger (ed.), *Salzschäden an Kulturgütern: Stand des Wissens und Forschungsdefizite; Ergebnisse des DBU Workshops im Februar 2008 in Osnabrück*, Hannover, 2009, p. 30–51.

Buralev and Balagurova 2021 I. Buralev and A. Balagurova*, Archaeological Iron Conservation: Theoretical Background of Finds Deterioration, Organization and Support of Preservation Activities*, in *Multidisciplinary Research in Archaeology*, 2 (https://doi.org/10.24412/2658–3550–2021–2–89–124), 2021, p. 89–124.

Chiantore and Lazzari 2001 O. Chiantore and M. Lazzari, *Photo–Oxidative Stability of Paraloid Acrylic Protective Polymers*, in *Polymer*, 42 (1) (https://doi.org/10.1016/S0032–3861(00)00327–X), 2001, p. 17–27.

Gerwin and Baumhauer 2000 W. Gerwin and R. Baumhauer*, Effect of Soil Parameters on the Corrosion of Archaeological Metal Finds*, in *Geoderma*, 96, 1–2 (https://doi.org/10.1016/S0016–7061(00)00004–5), 2000, p. 63–80.

Jaeger 2008 T. Jaeger, *Short Communication Removal of Paraffin Wax in the Re–Treatment of Archaeological Iron*, in *Journal of the American Institute for Conservation*, 47 (3) (https://doi.org/10.1179/019713608804539619), 2008, p. 217–223.

Knight 1982 B. Knight, *Why do some iron objects break up in store?*, in R.W. Clarke and S.M. Blackshaw (ed.), *Conservation of Iron, National Maritime Museum Monographs and reports*, 53, 1982, p. 50–51.

Lara *et al.* 2014 R. Lara, M. Monroy, M. Mallet, L. Dossot, M. González–Lozano and R. Cruz, *An experimental study of iron sulphides weathering under simulated calcareous soil conditions*, in *Environmental earth sciences*, 73 (https://doi.org/10.1007/s12665-014-3540-y), 2014, p. 1849–1869.

Loeper–Attia 2007 M.–A. Loeper–Attia, *A Proposal to Describe Reactivated Corrosion of Archaeological Iron Objects*, in *Corrosion of Metallic Heritage Artefacts*, Elsevier, 2007, p. 190–202.

Neff *et al.* 2004 D. Neff, S. Reguer, L. Bellot-Gurlet, P. Dillmann and R. Bertholon, *Structural Characterization of Corrosion Products on Archaeological Iron: An Integrated Analytical Approach to Establish Corrosion Forms*, in *Journal of Raman Spectroscopy*, 35 (8–9) (https://doi.org/10.1002/jrs.1130), 2004, p. 739–745.

North and MacLeod 1987 N.A. North and I.D. MacLeod, *Corrosion of Metals*, in C. Pearson (ed.), *Conservation of Marine Archaelogical Objects*, London, 1987, p. 68–98.

Ntelia and Karapanagiotis 2020 E. Ntelia and I. Karapanagiotis, *Superhydrophobic Paraloid B72*, in *Progress in Organic Coatings*, 139 (https://doi.org/10.1016/j.porgcoat.2019.105224), 2020, p. 1–4.

Organ 1977 R.M. Organ, *The current status of the treatment of corroded metal artefacts*, in B.F. Brown *et al.* (ed.), *Corrosion and Metal Artefacts, NBS Special Publication 479*, US Government Printing Office, Washington DC, 1977, p. 107–142.

Pingitore *et al.* 2015 G. Pingitore, T. Cerchiara, G. Chidichimo, M. Castriota, C. Gattuso and D. Marino, *Structural Characterization of Corrosion Product Layers on Archaeological Iron Artefacts from Vigna Nuova, Crotone (Italy)*, in *Journal of Cultural Heritage*, 16, 3 (https://doi.org/10.1016/j.culher.2014.07.003), 2015, p. 372–376.

Réguer, Dillmann and Mirambet 2007 S. Réguer, P. Dillmann and F. Mirambet, *Buried Iron Archaeological Artefacts: Corrosion Mechanisms Related to the Presence of Cl-Containing Phases*, in *Corrosion Science*, 49, 6, (https://doi.org/10.1016/j.corsci.2006.11.009) 2007, p. 2726–2744.

Réguer *et al.* 2007 S. Réguer, D. Neff, L. Bellot–Gurlet and P. Dillmann, *Deterioration of iron archaeological artefacts: micro-Raman investigation on Cl-containing corrosion products*, in *Journal of Raman Spectroscopy*, 38 (https://doi.org/10.1002/jrs.1659) 2007, p. 389–397.

Rérolle, and Lemeux–Fraitot 2025 C. Rérolle and S. Lemeux–Fraitot, *La collection métallique du musée Girodet après l'inondation du Loing, le 31 mai 2016*, in *Le Métal en danger – les dangers du Métal. Journée Métal France 2025. Protection & Conservation du Patrimoine Métallique, 7 Febr. 2025*, Toulouse, p. 25–30 and oral presentation.

Scarlett 2016 T.J. Scarlett, *Potential Applications of Supercritical Carbon Dioxide Extraction and Impregnation for the Stabilization and Conservation of Industrial Heritage Artefacts, Final Project Report*, Michigan Technological University, 2016.

Scott and Eggert 2009 D.A. Scott and G. Eggert, *Iron and Steel in Art: Corrosion, Colorants, Conservation*, London, 2009.

Selwyn 2021 L. Selwyn, *Understanding Flash Rusting* (https://www.canada.ca/en/conservation-institute.html), Canadian Conservation Institute, Ottawa, 2021.

Selwyn, Sirois and Argyropoulos 1999 L.S. Selwyn, P.J. Sirois and V. Argyropoulos, *The Corrosion of Excavated Archaeological Iron with Details on Weeping and Akaganeite*, in *Studies in Conservation*, 44, 4, 1999, p. 217–232.

Society for Museum Archaeology 2020 Society for Museum Archaeology, *Collections Packaging & Silica Gel. SMA Material Fact Sheet* (https://drive.google.com/file/d/1g–qGWaAm6VVRZEWl4kHmHbDI_r_SOMbA/view), 2020.

Tétreault 2021 J. Tétreault, *Products Used in Preventive Conservation*, in *Technical Bulletin 32* (https://www.canada.ca/en/conservation–institute/services/conservation–preservation–publications/technical–bulletins/products–used–preventive–conservation.html), Canadian Conservation Institute, Ottawa, 2021.

Thickett 2012 D. Thickett, Post Excavation Changes and Preventive Conservation of Archaeological Iron, Ph.D. Thesis, University of London, 2012.

Tradowsky *et al.* 2023 J.S. Tradowsky, S.Y. Philip, F. Kreienkamp, S.F. Kew, P. Lorenz, J. Arrighi, T. Bettmann *et al.*, *Attribution of the Heavy Rainfall Events Leading to Severe Flooding in Western Europe during July 2021*, in *Climatic Change* 176, 7 (https://doi.org/10.1007/s10584–023–03502–7), 2023, p. 1–38.

Turgoose 1982 S. Turgoose, *Post–excavation changes in iron antiquities*, in *Studies in conservation*, 27, 1982, p. 97–101.

Vinçotte *et al.* 2019 A. Vinçotte, E. Beauvoit, B. Nicolas Boyard and E. Guilminot, *Effect of Solvent on PARALOID® B72 and B44 Acrylic Resins Used as Adhesives in Conservation*, in *Heritage Science*, 7, 42 (https://doi.org/10.1186/s40494–019–0283–9), 2019, p. 1–9.

Wang 2007 Q. Wang, *An Investigation of Deterioration of Archaeological Iron*, in *Studies in Conservation*, 52 (2), 2007 (https://doi.org/10.1179/sic.2007.52.2.125), p. 125–134.

Watkinson, Rimmar and Emmerson 2019 D.E. Watkinson, M.B. Rimmer and N.J. Emmerson, *The Influence of Relative Humidity and Intrinsic Chloride on Post–Excavation Corrosion Rates of Archaeological Wrought Iron*, in *Studies in Conservation* 64, 8 (https://doi.org/10.1080/00393630.2018.1565006), 17 November, 2019, p. 456–471.

Wen *et al.* 2018 X. Wen, P. Bai, B. Luo, S. Zheng and C. Chen, *Review of recent progress in the study of corrosion products of steels in a hydrogen sulphide environment, in Corrosion Science*, 139 (https://doi.org/10.1016/j.corsci.2018.05.002) 2018, p. 124–140.

Williams 2019 R.S. Williams, Plastic Storage Products, in *Preventive Conservation: Collection Storage*, New York, 2019, p. 753–779.

Yanchyshyn 2022 Y. Yanchyshyn, *Common Packing Materials for Artworks* (https://www.icon.org.uk/static/fbec4eed–127c–4c21–9e86fbcd5c3f3fe8/681600d2–c8a6–4b0b–b15ff03ae6b9e028/Packing–Materials–List.pdf), The institute of Conservation (ICON UK), London, 2022.

NOTES

1. Barnich 2022.
2. Buralev and Balagurova 2021, p. 96-97; Selwyn 2021.
3. Bertholon (like several others) identified different states in the 'life of an archaeological object' after its creation and use in his research on the 'surface d'origine'. Bertholon 2000, p. 206-218.
4. Wang 2007, p. 131-132.
5. Scott and Eggert 2009, p. 146-147

6. Pingitore *et al.* 2015; Jaeger 2008; Brüggerhoff, Eggert and Simon 2009, p. 37; Scarlett 2016, p. 19-20; Ntelia and Karapanagiotis 2020, p. 1; Chiantore and Lazzari 2001, p. 17.

7. According to information on the customary conservation–restoration treatment procedures for metal conservation, via Cristel Cappucci.

8. Juprelle, Wanze, Renaud Castle, Herbeumont Castle, Poilvache, and Pommeroeul, see Annex (Table 1).

9. Loeper–Attia 2007.

10. Scarlett 2016, p. 7-8; Scott and Eggert 2009, p. 95-98, Thickett 2012, p. 24-31.

11. Objects CDC–LX–007790 and CDC–LX–007794.

12. Objects from Herbeumont Castle CDC–LX–007791–92, CDC–LX–007795–96, CDC–LX–007798; Wanze Golf CDC–LG–023378; Poilvache CDC–NR–015626; Pommeroeul CDC–HT–005280.

13. Objects from Poilvache CDC–NR–015624, CDC–NR–015625 and CDC–NR–015626.

14. Object from Juprelle CDC–LG–023380.

15. Tétreault 2021; Williams 2019.

16. Objects from Herbeumont Castle CDC–LX–007796 and CDC–LX–007795.

17. Object from Herbeumont Castle CDC–LX–007797.

18. Object from Herbeumont Castle CDC–LX–007794.

19. Leica, S9i stereoscope was applied by different magnifications.

20. Epoxy resin AY103, hardener HY956 charged with black pigments, according to information on the customary conservation–restoration treatment procedure from the metal conservator, via Cristel Cappucci, no conservation reports available.

21. Derived from the terms for the microstructure of a stratum from the MiCorr (Microstructure and corrosion database https://micorr.org/), Bertholon 2000, p. 274.

22. Scott and Eggert 2009, p. 99 and pl. 55.

23. Selwyn, Sirois and Argyropoulos 1999, p. 221-225; Brüggerhoff, Eggert and Simon 2009, p. 38-39.

24. Bertholon 2000, p. 269; Scott and Eggert 2009, p. 101-102.

25. Bertholon 2000, p. 275.

26. Bertholon 2000, p. 274.

27. Objects from Pommeroeul CDC–HT–005279, CDC–HT–005280; Juprelle CDC–LG–023380; Herbeumont Castle CDC–LX–007790, CDC–LX–007791, CDC–LX–007794, CDC–LX–007797; Renaud Castle CDC–LX–007799.

28. Organ 1977.

29. Knight 1982; Turgoose 1982.

30. SEM–EDX analysis performed with a ZEISS, Evo 15LS – Oxford Instruments, Aztec.

31. Selwyn, Sirois and Argyropoulos 1999, p. 220.

32. Turgoose 1982, p. 99.

33. Selwyn, Sirois and Argyropoulos 1999, p. 223.

34. µRAMAN analysis was done by Maaike Van Dorpe in the laboratories of KIK–IRPA with a RAMAN EnVia Qonton equipment (RENISHAW).

35. Neff *et al.* 2004; Réguer *et al.* 2007.

36. Réguer *et al.* 2007, p. 394, fig. 7.

37. Pingitore *et al.* 2015, p. 4.

38. Réguer *et al.* 2007, p. 389.

39. Scott and Eggert 2009, p. 63.

40. North and MacLeod 1987; Wen *et al.* 2018.

41. Lara *et al.* 2014, p. 1853.

42. Réguer, Dillmann and Mirambet 2007; Gerwin and Baumhauer 2000.

43. Oral consultation with actual CCE metal conservator Cristel Cappucci informed about the most common treatments applied on archaeological metal finds of the CCE collection in the past (22/09/2022, 25/10/2023, 12/03/2024).
44. Rérolle and Lemeux–Fraitot 2025.
45. *Ibidem.*
46. Brokerhof, Ankersmit and Ligterink 2017, p. 82, 85-86; Williams 2019, p. 753-754.
47. Williams 2019, p. 753-754.
48. Yanchyshyn 2022, p. 3-4; Society for Museum Archaeology 2020, p. 2.
49. Bertholon 2000, p. 251-252.
50. FTIR analysis was carried out by Maaike Van Dorpe with the aid of Louise Decq, both working at the KIK–IRPA Laboratories. FTIR spectra were acquired with a Bruker Hyperion 3000, coupled to a microscope. By averaging 64 spectra (4000 to 650 cm−1) with a resolution of 4 cm−1 for sample measurements and background, the Mercury–Cadmium–Telluride (MCT) detector provides an adequate signal–to–noise ratio. The spectra were acquired and processed using OPUS 7.2 FTIR software.

ABSTRACTS

In July 2021, heavy rainfall inundated the entire archaeological storage area of Namur's Centre de Conservation et d'Étude (CCE, AWaP), impacting part of the metal collection with contaminated water and mud. A selection of iron artefacts was examined to assess the damage and the factors contributing to this deterioration. Corrosion patterns and other surface phenomena were examined both macroscopically and microscopically. In addition to the typical orange pitting and exfoliation of the metallic layer, spherical (and broken) shells of dried droplets, along with liquid and dried phase formations, as well as orange–brown columns or curly corrosion products on the damaged iron surfaces, were observed. Unusual, elongated particles that appeared to grow upwards in a *stalactiform* corrosion morphology were also noted.
SEM–EDX, µRAMAN, and FTIR analyses revealed the presence of pyrrhotite and the active corrosion product akageneite. Great attention was devoted to understanding the interaction between metal corrosion and the materials used to package the archaeological objects, as well as the impact of previous conservation treatments. In particular, in objects wrapped in bubble wrap, the thin layer formed during the 'weeping iron' process exhibited extreme forms. Furthermore, unusual white deposits were noted, identified as various forms of CaCO3.
This study aimed to gain a deeper understanding of flood damage and subsequent conservation conditions and to reconsider the use of packaging materials for storage.

En juillet 2021, de fortes pluies ont inondé l'ensemble des dépôts archéologiques du Centre de Conservation et d'Étude (CCE, AWaP) à Namur, affectant une partie de la collection métallique par l'eau polluée et la boue. Une sélection d'objets en fer a été faite pour envisager les dommages et les facteurs contribuant à cette détérioration. Les formes de corrosion et autres phénomènes de surface ont été examinés à un niveau macroscopique et microscopique. En plus des piqûres orange typiques et de l'exfoliation de la couche métallique, des (fragments de) coques sphériques de gouttes séchées, des formations de phases liquide/séchée, ainsi que des colonnes orange–brun ou des produits de corrosion en forme de bouclette ont été observés sur les surfaces de fer

dégradées. Des particules allongées, une forme de corrosion semblant se développer vers le haut, ou stalactiforme, ont également été remarquées.
Les analyses SEM–EDX, µRAMAN et FTIR ont démontré la présence de pyrrhotite et du produit de corrosion actif, l'akaganéite. Une attention particulière a été portée à la compréhension de l'interaction entre la corrosion du métal et les matériaux utilisés pour emballer les objets archéologiques, ainsi qu'à l'influence des traitements de conservation antérieurs. En particulier sur les objets enveloppés dans du papier bulles, la fine couche formée pendant le processus de suintement du fer a pris des formes extrêmes. De plus, des dépôts blancs particuliers ont été observés et identifiés comme différentes formes de $CaCO_3$.
Cette étude vise à mieux comprendre les dommages causés par l'inondation et les conditions de conservation tout de suite après ce sinistre et de repenser l'utilisation des matériaux de conditionnement dans les dépôts archéologiques.

In juli 2021 zorgden hevige regenbuien ervoor dat de archeologische depots van het Centre de Conservation et d'Étude (CCE, AWaP) in Namen volledig overstroomden. Hierbij raakte een deel van de metaalcollectie aangetast door vervuild water en modder. Een aantal ijzeren artefacten was geselecteerd om de schade en de factoren die bijdragen aan deze degradatie te bestuderen. Corrosiepatronen en andere oppervlakteverschijnselen werden op macroscopisch en microscopisch niveau onderzocht. Op de ijzeren oppervlakken kwamen diverse schadefenomenen voor: typische oranje putvorming en exfoliatie van de metaallaag, bolvormige (en gebroken) schalen van opgedroogde druppels, het ontstaan van vloeibare/droge fasen, oranje–bruin gekleurde zuiltjes en krullende corrosieproducten. Ongebruikelijke langwerpige deeltjes, die schijnbaar opwaarts leken te groeien en zo een stalactietvormig corrosieproduct ontwikkelden, zijn ook waargenomen.
SEM–EDX, µRAMAN en FTIR–analyses onthulden de aanwezigheid van pyrrhotiet en het actieve corrosieproduct akaganeïet. Bijzondere aandacht ging naar de interactie tussen de metaalcorrosie en de verpakkingsmaterialen van de archeologische objecten, evenals de invloed van eerdere conserveringsbehandelingen. Vooral bij objecten gewikkeld in noppenfolie nam de dunne laag, ontstaan tijdens het 'weeping iron'–proces, uitzonderlijke verschijningsvormen aan. Bovendien konden opmerkelijke witte afzettingen worden geïdentificeerd als verschillende vormen van $CaCO_3$.
Dit onderzoek had als doel de schade, veroorzaakt door de overstroming en de daaropvolgende bewaaromstandigheden, beter te begrijpen en na te denken over het gebruik van verpakkingsmaterialen in depots.

INDEX

Keywords: archaeological iron, flooding damage phenomena, iron corrosion, akageneite, weeping iron
Trefwoorden archeologisch ijzer, overstromingsschadefenomenen, ijzercorrosie, akaganeïet, huilend ijzer
Mots-clés: fer archéologique, phénomènes de dégradation liés aux inondations, corrosion du fer, akaganéite, suintement du fer

AUTHORS

ELKE OTTEN

Elke Otten holds an MA in History from the University of Ghent (UGent) and another in Metal Restoration from the University of Antwerp (UAntwerpen). She has worked as a conservator–restorer and collection manager at the archaeological laboratory of the Brussels Capital Region and the War Heritage Institute. She was part of the preventive conservation unit at the Royal Institute for Cultural Heritage (KIK–IRPA) until 2025, and is currently responsible for collection management at the Royal Museums of Fine Arts of Belgium (RMFAB).

HELENA WOUTERS

Helena Wouters earned her doctoral degree in Chemistry from the University of Antwerp (UAntwerpen). She is a senior scientist at the Metals and Glass Laboratories of the Royal Institute for Cultural Heritage (KIK–IRPA), where she has accumulated over 30 years of experience in Heritage Science analysis. From 1993 to 1998, she served as an invited professor in the Conservation and Restoration section of the Antwerp Polytechnic, now part of the University of Antwerp.

ANNE–SOPHIE BARNICH

Anne–Sophie Barnich
holds a master's degree in Art History and Archaeology from University of Brussels (ULB). Since 2010, she has trained in preventive conservation at the Prehistomuseum and the conservation and study centre of the Walloon Heritage Agency. Since 2020, she has managed the archaeological collections for the Centre de Conservation et d'Étude (CCE, AWaP).